GEOSCIENCES

Increase in the number of explosive low–level cyclones around King George Island in the last three decades

ALBERTO W. SETZER, MARY T. KAYANO, MARCELO R. OLIVEIRA, WILMAR L. CERÓN & MARCELO B. ROSA

Abstract: This paper documents an increase in the number of observed explosive cyclones (EC) at King George Island, South Shetland Islands, Antarctica, over the 1989–2020 period. In ECs at 60° latitudes the surface atmospheric pressure drops ≥24 hPA in 24 hours. The annual EC frequency time series shows a significant positive trend of ~2.7 cyclones/ decade, with a break in 2003 and average numbers of 7.3 and 11.8 events before and after that break, respectively. The increase follows closely earlier documented global sea surface temperature (SST) anomaly trends for the 1981–2018 period, partially attributed to global warming and to the Pacific Decadal Oscillation (PDO). Connections between EC frequency and SST might occur through variations in SST in the southeastern Pacific and southwestern Atlantic, with anomalous cold conditions favoring an increase in ECs. We also found close relations between the number of ECs with simultaneous occurrences of PDO and Atlantic multidecadal oscillation in opposite phases, so that after 2003 they were in the cold and warm phases, respectively, and vice-versa before 2003. Both low-frequency modes seem to modulate the number of ECs. As per the authors knowledge these results have not been discussed before and may help climate modeling studies and weather forecasts.

Key words: explosive cyclones, climate variability, sea surface temperature, trends, low-frequency variability.

INTRODUCTION

Systems with high destructive power associated to strong winds, heavy rainfall and damaging storm surges are becoming more frequent under climate change (Houghton 1990). One of them is the explosive low-level cyclone, also known as a meteorological "bomb" or "explosive" (hereafter EC), which in general has a maritime character and is more frequent during the cold season. An extratropical surface cyclone is classified as explosive when it deepens rapidly with the migration of its core pressure at surface level resulting in more than 24 hPa drop in 24 hours. This ratio of pressure drop over time originated the Bergeron "B" scale, with three categories defined: "weak" for 1≤B<1.3, "moderate" for 1.3≤B<1.9, and "strong" for B≥1.9; additionally, the ratio value is multiplied by a local latitude factor, (sin latitude/sin 60°), thus reaching its minimum at the poles (Sanders & Gyakum 1980). Despite their destructive feature, a few studies can be found in the literature regarding the Southern Hemisphere (SH) ECs compared to those observed in the Northern Hemisphere. These studies focused on the synoptic conditions leading to the development of the ECs in specific regions, such as Argentina (Seluchi & Saulo 1998) and the New South Wales coast (Speer et al. 2009), and their climatological

features (Sinclair 1995, 1997, Lim & Simmonds 2002, Black & Pezza 2013). The EC cyclogenesis is more frequent at the 45°S–50°S sector of the South Indian and Atlantic Oceans (Sinclair 1995, 1997). Whereas a maximum EC density occurs to the south of Australia and the New Zealand region, signs of these systems in the Pacific up to the Drake Passage are relatively weak (Lim & Simmonds 2002).

Using weather station data from 1991 to 2007 Romão & Setzer (2008) analyzed ECs that crossed the ~1,000 km wide Drake Passage in the SE direction and reached King George Island usually in about 12 hours; the EC "season" with 44% of the cases, concentrated in the July–September period, peaking in September. The average number of cases per year increased from five or six to twelve, and strong ECs in Bergeron scale occurred in Aug/99 and March/2003, with a pressure drop of ~44 hPa in 24 h for both cases, with the lowest pressures of 965.1 hPa and 958.7 hPa and wind gusts of ~39 m/s and ~47 m/s, respectively. Hurricane-force cyclones and ECs in the Drake Passage have been known since the European navigation started in the region in the 1500s, producing the world´s highest shipwreck numbers until the Panama Canal opened in 1904. Ensuing sea conditions in the region may include "rogue" or "freak" waves of some 30m causing severe damage to large and solid ships as was the case with the Bremen in February/2001 and with Caledonian Star in March/2001 (ESA 2004). "Screaming Sixties" is a common reference to the Southern latitude belt with its powerful cyclones and sea waves (Toffoli & Aeria 2017).

A recent EC reached King George Island on April 14-15/2021, with a 43.4 hPa drop in 24 hours at the Chilean Frei weather Station (WMO # 89056), therefore a 1.8 Bergeron moderate and almost strong EC; its maximum drop was 10.5 hPa in three hours. It was a record Bergeron for

April since 1989, with 29.5 m/s wind gusts and 22.5 m/s sustained winds, but falling short of the 49.8 hPa record drop on 22/July/2013. An animation of this EC with satellite images is presented at WEC (2021) and, Figures 1a and 1b show the synoptic conditions and a satellite picture depicting this event.

The EC frequency seems to be changing over the last decades. Lim & Simmonds (2002) found a statistically significant positive trend in the global EC numbers, with the a SH increase of 0.56 EC/year during the 1979–1999 period. They used the National Center for Environmental Prediction–Department of Energy (NCEP–DOE) Reanalysis II dataset. Befort et al. (2016) highlighted that the number of ECs in the SH with core pressure below 960 hPa depends on the dataset and period of analysis, based on results using the National Oceanic and Atmospheric Administration (NOAA) 20th Century Reanalysis (NOAA–20CR) and the 20th Century ECMWF Reanalysis (ERA–20C). They found a positive trend from 1920 to 2000 for the NOAA–20CR, and a local maximum by 1940 between two local minima, one at the beginning of the 20th century and the other by 1960 for the ERA–20C.

Nevertheless, the SH EC frequency dependence on the period of analysis might also indicate modulations by low-frequency variability modes. In this context, Simmonds & Keay (2000) suggested that the negative trend in the number of extratropical cyclones after 1970 is explained by the SH warming associated with the decadal to multidecadal sea surface temperature (SST) variability. Modeling studies indicated that the SST decadal modes alter the baroclinicity in the SH extratropics and, consequently, the number of SH extratropical cyclones increases in the 40°S–55°S latitudinal band and decreases poleward south of it (Reason & Murray 2001). In this line, Lopez et al. (2016) showed that the SST anomalies in the tropical
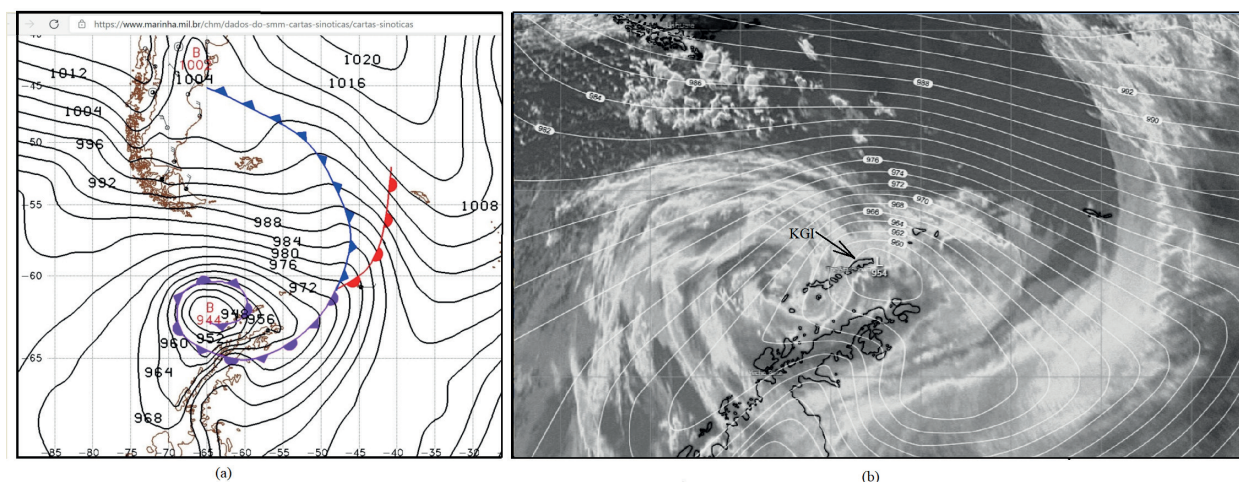
Figure 1. (a) Synoptic surface analysis for 15/April/2021 00h UTC showing an EC with ~944 hPa at its center and strong pressure gradients in the south of the Drake Passage, approaching King George Island from the east (chart from the Brazilian Navy and available at https://www.marinha.mil.br/chm/dados-do-smm-cartas-sinoticas/ cartas-sinoticas). (b) Satellite infrared image at 15/April/2021 02:30h UTC with the EC low pressure center at 954 hPa slightly East of King George Island (extracted from www.windy.com/ on 14 and 15/April/2021).

Pacific associated with the interdecadal Pacific oscillation mode are negatively correlated with the SST anomalies in the southwestern Atlantic (south of 40°S around the King George Island), and positively with the SST anomalies in the Amundsen Sea.

The Atlantic multidecadal oscillation (AMO) (Kerr 2000, Enfield et al. 2001) is another climate variability mode that causes persistent SST anomalies in the extratropical Southern Oceans (Folland et al. 1999), as noted in the Weddell Sea SST (Crowley & Kim 1993). Kayano et al. (2019) suggested that the AMO, through changes in the meridional SST gradient, modulates the baroclinicity in the South Atlantic and southeastern Pacific midlatitudes, which increases when the SST gradient is northward during the warm AMO (WAMO) phase, and decreases when the SST gradient is in the opposite direction during the cold AMO (CAMO) phase; they also showed that the low-level extratropical cyclones in the southeastern Pacific and South Atlantic are more energetic in the WAMO (2003–2017) than in the CAMO (1979–1993).

It is likely that the more energetic extratropical cyclones also have more potential to evolve into ECs than the less energetic ones. This hypothesis can be tested by detecting ECs in the Southern Oceans during the two AMO phases. Fortunately, in situ counts of ECs at the Brazilian Comandante Ferraz Antarctic Station (62° 05' 07'' S; 58° 23'33'' W, WMO #89252) located in the Admiralty Bay, King George Island (henceforth, Ferraz Station), South Shetland Islands, have been undertaken operationally from 1989 until 2010; after that, hourly records from the Chilean Frei weather station (WMO #89056) at the same island were used. The period starting in 1989 up to the present overlaps the CAMO and the WAMO phases and therefore, this in situ observed EC frequency time series provides a unique opportunity to address the above question. Besides, the cyclone monitoring task also has obvious importance directly related to the safety of ships and activities in general in the region. All these reasons motivated us to investigate the trends and variability of the EC frequency time series at King George Island and their possible causes.

MATERIALS AND METHODS

Monthly SST data were obtained from the extended reconstructed SST version V5 dataset (Huang et al. 2017) for grid points with 2° horizontal resolution and available at the National Oceanic and Atmospheric Administration (NOAA)'s website psl.noaa.gov/data/gridded/. Global SST data were obtained for the 1989–2020 period. The SST data were also obtained in two areas, one in the Atlantic (equator, 20°N, 60°W, 0° Greenwich longitude), and another in the Pacific (equator, 20°N, 150°W, 80°W) for the 1951–2020 period.

Monthly numbers of ECs were obtained from the hourly records of atmospheric pressure and weather data at the stations of Ferraz(WMO #89252) from 1989 until 2010, when it ceased operating (INPE 2021), and Frei (WMO #89056) after 2010. As part of the its operational procedures all 89252 sensors and associated electronics with automatic recording were calibrated every summer and repaired or replaced if needed. In the case of atmospheric pressure, two routines were always used to calibrate the automatic records. First, against those of the own station´s Mercury precision barometer with readings compensated for air temperature, elevation and latitude. Second, comparison with records of the various weather stations at King George Island, in particular with those from the Chilean Frei (WMO #89056) and its neighbouring Russian Bellingshausen (WMO #89050) stations, both distant 33 km from Ferraz; in this case, the synoptic charts were also used to select conditions with no pressure gradient in the area. Differences found among the stations were always within the uncertainty specified by the instrument´s manufacturer.

First, the annual time series of the number of EC events was examined for a linear trend. The significance of this time series trend was tested using the statistical non-parametric Mann–Kendall test (Mann 1945, Kendall 1975). The time series linear trend was calculated using Sen's slope (β) estimator (Theil 1950, 1992, Sen 1968). The change point in the time series was obtained using Pettitt's test (Pettitt 1979), which identifies changes in the mean and when a rupture occurs. In this test, the null hypothesis (H_0) that no rupture exists in the time series is tested against the alternative hypothesis (H_1), with changes in the mean. The significance levels α = 0.1 (90%) and α = 0.05 (95%) were used in this test. Given that the null hypothesis is assumed to be true, α is the significance level and is the probability of the test rejecting the null hypothesis.

Next, the relation of the monthly EC frequency time series to the global SST variability patterns were examined considering simultaneous correlation maps. First, monthly standardized SST anomalies were calculated. These anomaly time series contain trends, so that they are referred to as SST anomalies with trend. In another approach, prior to any calculation, the linear trend was removed from the SST time series using the least square method, producing monthly standardized SST anomalies, which became the detrended anomalies. Also, the corresponding detrended monthly EC frequency time series was obtained. In these calculations, trends, monthly means, and standard deviations were for the 1989–2020 base period. Before the correlation calculations, the time series were smoothed with a 61–month running means filtering order to remove the high-frequency variability. The correlation maps were obtained by correlating the monthly EC frequency time series and the SST anomaly time series with trend, as well as for the detrended EC frequency time series with the detrended SST anomaly time series. The Pearson's correlation coefficient (r) was used and the correlation

statistical significance was assessed with the Student's t-test at a 95% confidence level (Panofsky & Brier 1968).

Analyses of the correlation map for the detrended time series indicate key areas for which the SST anomalies were closely related to the EC frequency time series. It will be shown in the results that two target areas were identified, being those abovementioned and for which the SST data were selected in the 1951–2020 period. For each area, monthly detrended standardized SST anomalies were obtained considering the 1951–2020 base period. An SST anomaly index is defined as the difference between the averaged SST anomalies in two areas, one in the Atlantic (60°W, 0°E, 20°N, equator), and other in the Pacific (150°W, 80°W, 20°N, equator), considering Atlantic minus Pacific values, henceforth called Atlantic minus Pacific SST index (AP–SST). The reason to use a longer period for this index than that for the EC frequency was to avoid biases in this index due to the time series shortness. For instance, the trend removed in the AP–SST index was based on the 1951–2020 base period, where the climate change-related trend was removed. The AP–SST index was compared with the EC frequency time series from visual inspection and cross-wavelet analysis for the 1989–2020 period (Torrence & Webster 1999).

RESULTS

Variations in the number of ECs

ECs that migrate through the Drake Passage to King George Island occur throughout the year. Still, their frequency shows a seasonal variation with the highest values from July to September (maximum in August) and the lowest values during the summer months (minimum in January) (Figure 2). This result indicates that the EC is mainly a wintertime system with the second largest value in September.

The time series of the annual number of the ECs during the 1989–2020 period illustrated in Figures 3a and 3b was subjected to the Mann–Kendall test, showing a significant positive linear trend of 0.27 cyclones per year. This linear trend means an increase of almost three ECs per decade. However, the time series also shows a significant break in 2003, such that the average annual number before this break of 7.3 ECs contrasts with an average annual number of 11.8 ECs after the break, despite a reduced number of events in 2014 (Figures 3a and 3b). The time evolution of the annual number of ECs shows before the break only one maximum in 1999 exceeding 10 events, and after the break, three accentuated maxima exceeding 14 events in 2004, 2010, and 2011. This temporal variation in the number of ECs suggests the effects of the low-frequency variability modes, such as the Pacific decadal oscillation - PDO (Mantua et al. 1997) and the AMO. The PDO changed phase from its warm to cold phase by 1998–2000 (Hare & Mantua 2000) and the AMO, from its cold to warm phase, by 1997 (Frajka–Williams et al. 2017). However, these two low-frequency variability modes take at least 2–3 years to be completely established. Also, there is a multidecadal negative correlation between the tropical Pacific and Atlantic, such that WAMO relates to the CPDO and CAMO relates to the WPDO (Kucharski et al. 2016, Kayano et al. 2020). Furthermore, Kayano et al. (2019) suggested that the low-level extratropical cyclones in the southeastern Pacific and South Atlantic are more energetic during the WAMO than during the CAMO phase. These earlier outcomes indicate that the break in the annual number of EC's in 2003 does not coincide with the AMO and PDO phase change but occurs when both WAMO and CPDO were completed, established, and connected in a multidecadal time scale.
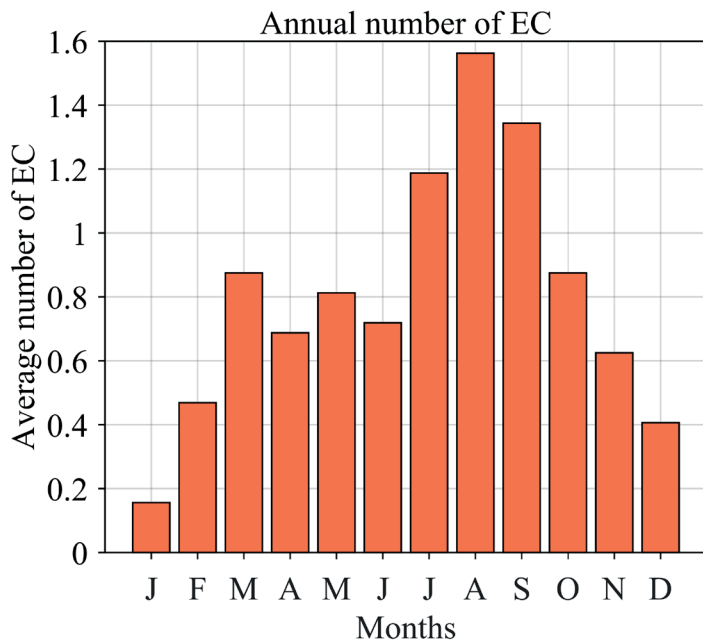
Figure 2. Monthly numbers of observed ECs at King George Island. Averages of the 1989–2020 period.
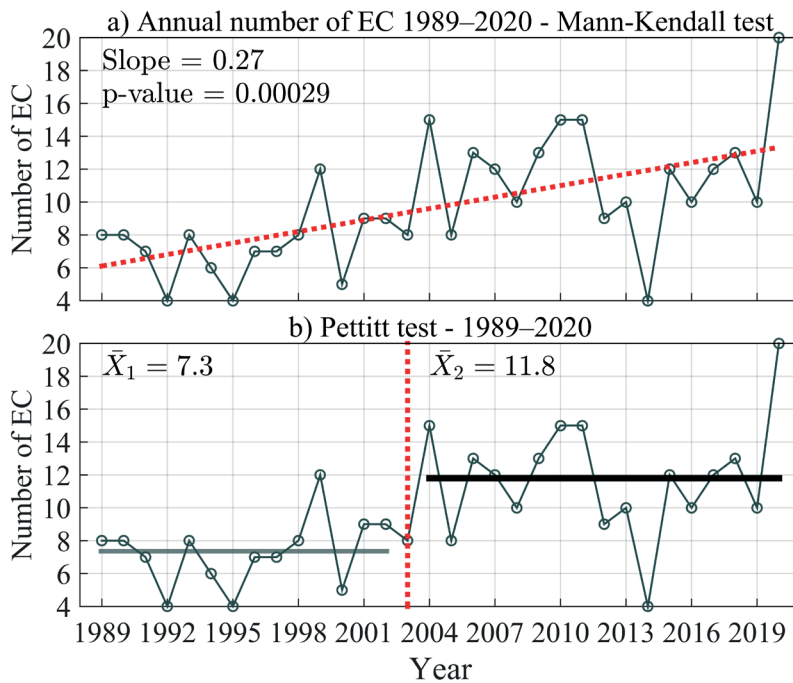

Figure 3. (a) Annual number of ECs observed at King George Island for the 1989-2020 period of 30 years and its linear increase rate of ~ 2,7 ECs/decade (red dotted line). (b) The ECs separated by the break year of 2003 (vertical red dashed line) at the 0.01 significance level; the two horizontal lines represent the average number of ECs prior ($\bar{X}_1$) and after ($\bar{X}_2$) the break.

Relations between ECs and SST anomalies

Figure 4 illustrates the correlation between the monthly EC frequency time series and SST anomalies with trend. This map reproduces the SST anomaly trend patterns for the 1981–2018 period documented by Bulgin et al. (2020) and the pressure data originated from official WMO stations with calibrated instruments. They provided a global pattern of the SST anomaly trend for the 1981–2018 period relative to the climatology of the 1982–2010 period. In their Figure 1a, positive trends occur in most of the Atlantic Ocean, tropical Indian Ocean, and in a horseshoe-shaped area in the western Pacific,

contouring smaller positive trends to weak negative trends in the tropical eastern Pacific; they also indicated a negative trend in most of the southern Oceans to the south of 50°S, with largest negative trends from the dateline to the southwestern Atlantic. Comparisons between our Figure 4 with their Figure 1a indicate close spatial correspondences between the trend signs with the correlation signs. So, the negative SST anomaly trends in the southeastern Pacific and part of southern Atlantic noted in the last 30 years (Bulgin et al. 2020) are most likely the main driver of the increase in the number of ECs at the King George Island.

Nevertheless, the EC frequency time series also presents interannual to multidecadal variability, as indicated by the break in 2003. These relations are illustrated in the correlation map between the detrended EC frequency time series and the detrended SST anomalies (Figure 5). Considering the correspondence of the signs of the correlations with the signs of the SST anomalies, the equatorial and North Atlantic

correlation pattern resembles the SST anomaly pattern during the WAMO, and that in the eastern Pacific the SST anomaly pattern during the cold PDO (CPDO) phase. The interpretation is that after the 2003 break the large average number of ECs, 11.8, was associated with the simultaneous occurrence of WAMO and CPDO. Before the break, the reduced average number of ECs, 7.3, was linked to the simultaneous occurrence of CAMO and warm PDO (WPDO). The dynamics involved in the simultaneous occurrences of AMO and PDO in opposite phases has been discussed earlier (Kucharski et al. 2016, Kayano et al. 2020). The AMO and PDO are linked in a multidecadal time scale through an east-west cell along the tropics with ascending motions in the warm side and descending motions in the cold side, where the easterlies are accelerated, which in turn further maintains the cold condition (Kayano et al. 2020). The 3-year delay in the break in the annual number of ECs in relation to the AMO and PDO phase changes indicates that the increase in the number of ECs occurs when the WAMO
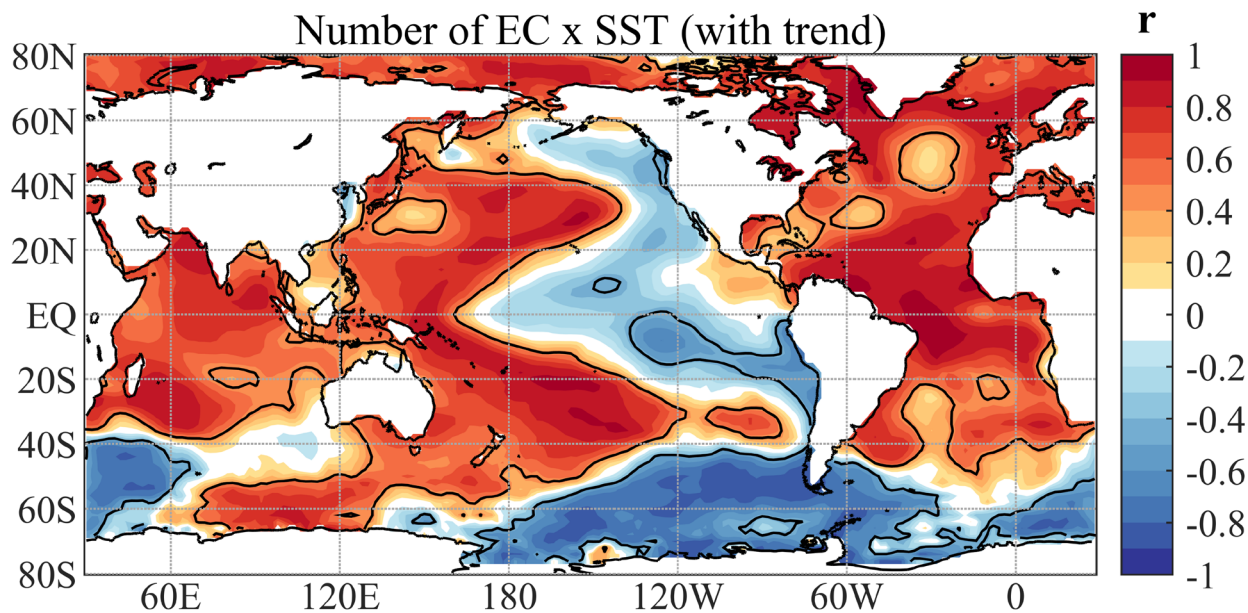

Figure 4. Correlation map between EC frequency time series and SST anomalies. Before the correlation calculations, the time series were filtered with a 61–month running means filter. The continuous line encompasses significant correlations at the 95% confidence level using the Student's t-test.

and CPDO are completely established and the multidecadal time scale dynamics connecting the Pacific and Atlantic is active.

Atlantic minus Pacific SST (AP–SST) index and the EC frequency time series

A visual inspection of the AP–SST index and the EC frequency time series indicate their close relationship from interannual to multidecadal time scales (Figure 6). Evidently these time series are too short to identify multidecadal relations. Nevertheless, their nearly synchronous variations over the analysis period provide a clue that a multidecadal relation might exist (Figure 6). The correlation between the two-time series is 0.83. Also, the time series are short to identify their phase relations in a time scale longer than decadal. The cross-wavelet analysis between the time series provides interesting relations at two interannual time scales. Indeed, significant coherence occurs during the 1990–2000 period at a 4–5 year time scale and a phase difference

of 90°, which implies that the maximum in the AP–SST occurs 1–1.2 year before the minimum in the index of EC frequency time series (Figure 7). Also, significant coherence occurs during the 2004–2020 period at a 6–8 year time scale and a phase difference of 45°, which means that the maximum in the AP–SST precedes the minimum in the EC frequency time series by 0.75–1 year (Figure 7). Interestingly, the break in the EC frequency time series occurs between these two periods. This means that the break separates the EC frequency time series in two periods related to the SST variability in the tropical eastern Pacific and North Atlantic, at two distinct interannual time scales. The results here indicate that the interannual relationships between the AP-SST index and the EC frequency time series are indeed modulated by the low-frequency variability of the Pacific and Atlantic Oceans.
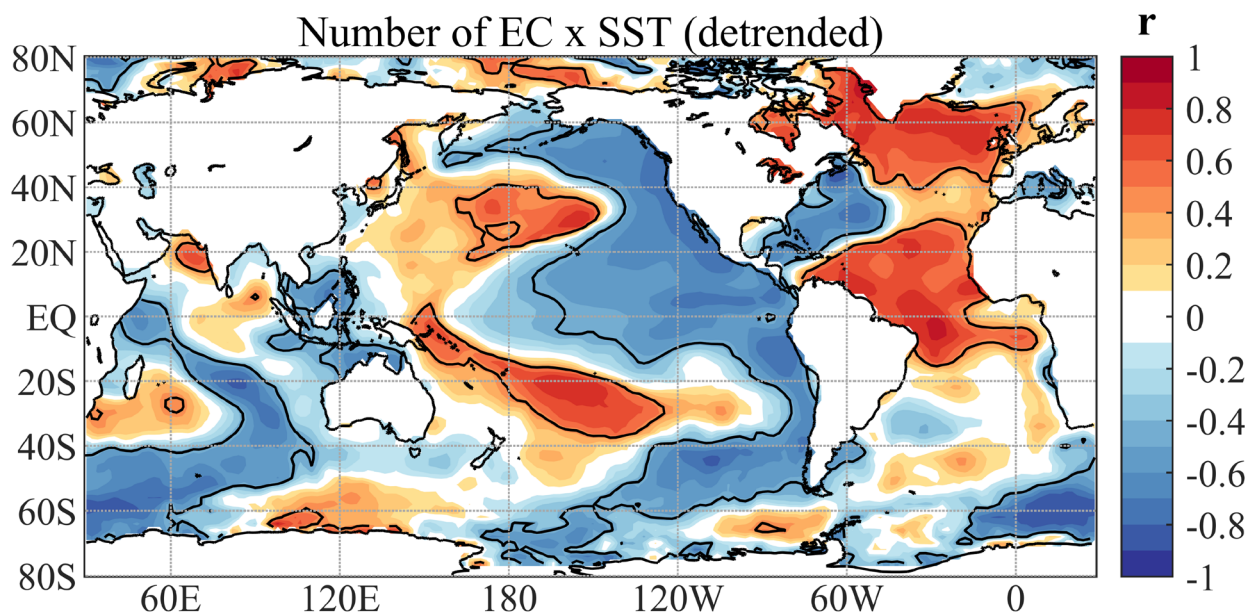

Figure 5. Correlation map between detrended EC frequency time series and detrended SST anomalies. Before the correlation calculations, the time series were filtered with a 61–month running means filter. The continuous line encompasses significant correlations at the 95% confidence level using the Student's t-test.
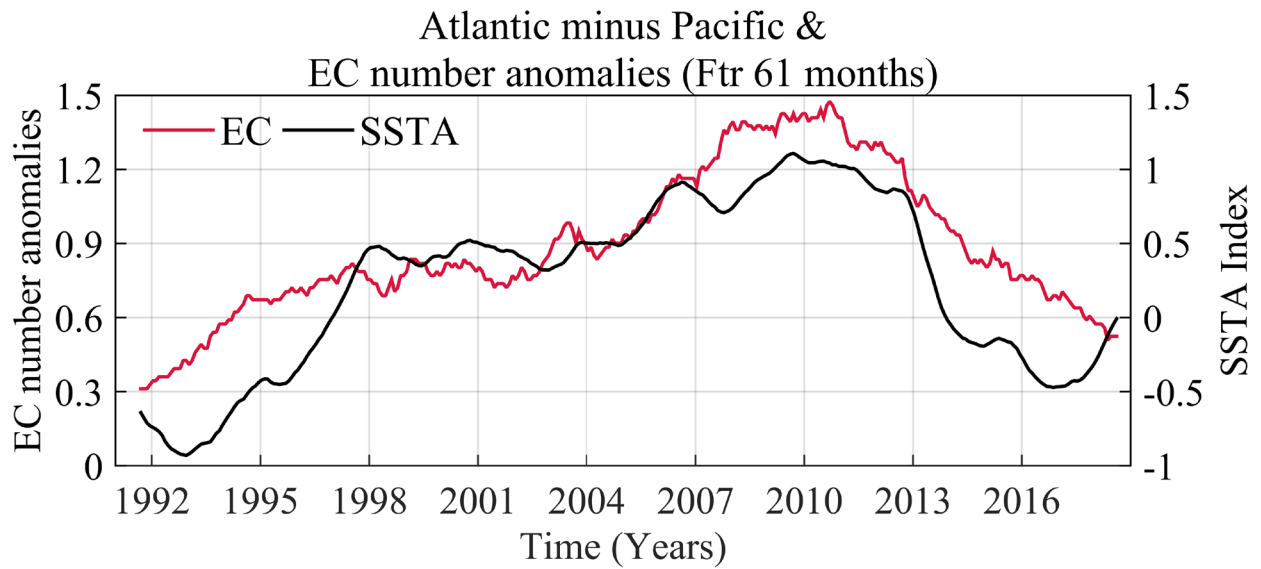
Figure 6. AP–SST index and number of ECs. Both time series were filtered with a 61–month running mean filter.
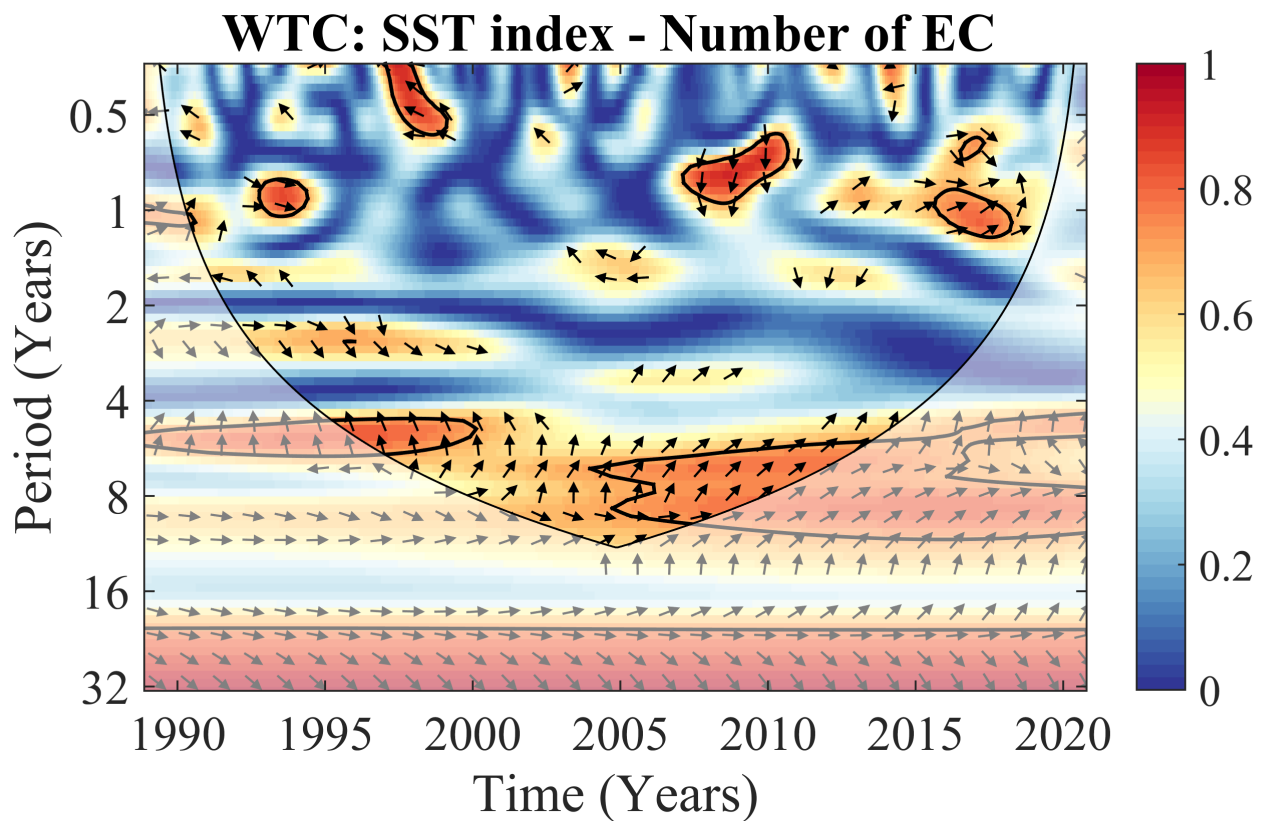

Figure 7. Wavelet coherence and phase differences between the AP–SST index and EC frequency time series during the 1989–2020 period. Closed contours are the squared wavelet coherence. The region where the edge effects are significant is under the U–shaped curve (cone of influence). The arrows indicate the phase differences as follows: in-phase (0°), pointing out to the right; out of phase (180°), pointing out to the left; the first-time series leading the second by 90°, pointing out down; and the first time series lagging the second by 90°, pointing upwards.

DISCUSSION

The time series of the observed annual number of ECs at the Drake Passage and King George Island during the 1989–2020 30-year period shows a significant positive linear trend of 0.27 cyclones per year (Figure 3a), plus a statistically significant break in 2003 that defines average numbers of 7.3 and 11.8 ECs, respectively, prior and after that year (Figure 3b). This break also separates the EC frequency time series in the 1990–2000 and 2004–2020 periods, when the interannual variabilities present significant coherencies with the AP–SST index (defined by the SST anomalies in the North Atlantic and eastern Pacific between the equator and 20°N), respectively at 4–5 year and 6–8 year time scales (Figure 7). Therefore, the break in 2003 highlights the change in the mean number of EC events and indicates that low-frequency variability modes might modulate such change with signatures in the tropical eastern Pacific (PDO) and North Atlantic (AMO).

Consistent with this hypothesis, the break year is close to the period when both low-frequency modes changed phases: the WPDO changed to the CPDO phase by 1998–2000 (Hare & Mantua 2000), and the CAMO changed to WAMO by 1997 (Frajka–Williams et al. 2017). This hypothesis was further explored here analyzing correlations between the EC frequency time series and SST anomalies over the globe with and without removing linear trends in the time series. The analysis without removing the linear trends reproduced most features of the trend SST anomaly pattern for the 1981–2018 period earlier documented (Bulgin et al. 2020), such that the signs of the correlations correspond with the signs of the trends (Figure 4). Although uncertainties on the data and method of analyses should be considered when trends are discussed in terms of a climate change point of view, the warming trends in the tropical Indian Ocean, most of the Atlantic and western Pacific (Bulgin et al. 2020) are consistent with those previously documented in the Intergovernmental Panel on Climate Change-IPCC reports (Hartmann et al. 2013, Pachauri & Meyer 2014). According to Bulgin et al. (2020), the South Pacific cooling trend might be related to the PDO. In the present analysis, the corresponding negative correlations extend from the dateline to the southwestern Atlantic, approximately to south of 40°S. Furthermore, the cooling trend in the southern extratropical Atlantic Ocean is a feature associated with the WAMO (Folland et al. 1999, Kayano et al. 2020). Thus, the increasing trend in the EC frequency during the 1989–2020 period might also reflect the low-frequency effects.

In this regard, the correlation map for the detrended time series (Figure 5) reproduced the SST anomaly pattern previously documented when both CPDO and WAMO occur simultaneously (Kayano et al. 2020). The interpretation is that after the break in 2003, the large average number of ECs, 11.8, was associated with the simultaneous occurrence of WAMO and CPDO, and before the break the reduced average number of ECs, 7.3, was linked to the simultaneous occurrence CAMO and warm PDO (WPDO). Consistent with this interpretation, Kayano et al. (2019) showed that the extratropical cyclones in the southeastern Pacific and South Atlantic are more energetic during the WAMO than during the CAMO. So, more energetic extratropical cyclones might more easily evolve into a EC category. The 3-year delay in the break in the annual number of ECs in relation to the AMO and PDO phase changes indicates that the increase in the number of EC's occurs when the WAMO and CPDO are completely established and connected in a multidecadal time scale dynamics of the Pacific and Atlantic Oceans (Kucharski et al. 2016, Kayano et al. 2020).

The Southern Annular mode effects on the EC's characteristics and trends have also been evaluated. No consistent relations have been found. Indeed, a figure similar to Figure 7 was constructed using the Antarctic Oscillation index. The correlation of this index and of the EC's frequency is close to zero. Although the ECs originate in extratropics, the analysis made indicates that once formed, their characteristics are not modulated by the AAO.

The present analysis provides observational evidence that the increase in the number of ECs at King George Island follows closely the global SST anomaly trends, which were partially attributed to global warming and partially to the low-frequency variability modes, the PDO and AMO. This connection seems to occur through the SST variations in the southeastern Pacific and southwestern Atlantic, such that an anomalous cooling favors the increase in the number of ECs. Projected increases in the number of extratropical cyclones have been predicted (Chang 2017), and to the best knowledge of the authors the results presented here have not been examined before and might be useful for future climate modeling and diagnostic studies and for forecasts of extreme weather brought by ECs in the Drake Passage and King George Island area. And as an update added in this text´s final proofreading, ECs numbered 14 in 2021 and five in the 2021-22 summer, the latter being the highest value since 1985, thus further confirming the increase trend of ECs in the region.

Acknowledgments

REFERENCES

BEFORT DJ, WILD S, KRUSCHKE T, ULBRICH U & LECKEBUSCH GC. 2016. Different long–term trends of extra-tropical cyclones and windstorms in ERA–20C and NOAA-20CR reanalyses. Atmos Sci Lett 17: 586-595. https://doi.org/10.1002/asl.694.

BLACK MT & PEZZA AB. 2013. A universal, broad- environment energy conversion signature of explosive cyclones. Geophys Res Lett 40: 452-457. https://doi.org/10.1002/grl.50114.

BULGIN CE, MERCHANT CJ & FERREIRA D. 2020. Tendencies, variability and persistence of sea surface temperature anomalies. Sci Reports 10: 7986. https://doi.org/10.1038/s41598-020-64785-9.

CHANG EKM. 2017. Projected significant increase in the number of extreme extratropical cyclones in the Southern Hhemisphere. J Clim 30: 4915-4935. http://dx.doi.org/10.1175/JCLI-D-16-0553.s1.

CROWLEY TJ & KIM K-Y. 1993. Towards development of a strategy for determining the origin of decadal-centennial scale climate variability. Quart Sci Rev 12: 375-385. https://doi.org/10.1016/S0277-3791(05)80003-4.

ENFIELD DB, MESTAS-NUÑEZ AM & TRIMPLE PJ. 2001. The Atlantic multidecadal oscillations and its relation to rainfall and river flows in the continental U.S. Geophys Res Lett 28: 2077-2080. https://doi.org/10.1029/2000GL012745.

ESA - THE EUROPEAN SPACE AGENCY. 2004. Ship-sinking monster waves revealed by ESA satellites. Available at https://www.esa.int/Applications/Observing_the_Earth/Ship-sinking_monster_waves_revealed_by_ESA_satellites. Accessed 19/April/2021.

FOLLAND CK, PARKER DE, COLMAN AW & WASHINGTON R. 1999. Large-scale modes of ocean surface temperature since the late nineteenth century. In: NAVARRA A (Ed), Beyond El Niño: decadal and interdecadal climate variability, 1st ed., Germany: Springer-Verlag Berlin Heidelberg, p. 73-102.

FRAJKA-WILLIAMS E, BEAULIEU C & DUCHEZ A. 2017. Emerging negative Atlantic Multidecadal Oscillation index in spite of warm subtropics. Sci Reports 7: 11224. https://doi.org/10.1038/s41598-017-11046-x.

HARE SR & MANTUA NJ. 2000. Empirical evidence for North Pacific regime shifts in 1977 and 1989. Prog Oceanogr 47: 103-146. https://doi.org/10.1016/S0079-6611(00)00033-1.

HARTMANN DL ET AL. 2013. Observations: Atmosphere and Surface. In: INTERGOVERNMENTAL PANEL ON CLIMATE CHANGE, Climate change 2013 the physical science basis:

Working group I contribution to the fifth assessment report of the intergovernmental panel on climate change, United Kingdom: Cambridge University Press, p. 159-254. https://doi.org/10.1017/CBO9781107415324.008.

HOUGHTON JT, JENKINS GJ & EPHRAUMS JJ. 1990. Climate Change: The IPCC Scientific Assessment. Report prepared for Intergovernmental Panel on Climate Change by Working Group I. Cambridge, New York, Port Chester, Melbourne & Sydney: Cambridge University Press, 410 p.

HUANG B, THORNE PW, BANZON VF, BOYER T, CHEPURIN G, LAWRIMORE JH, MENNE MJ, SMITH TM, VOSE RS & ZHANG H-M. 2017. Extended reconstructed sea surface temperature, version 5 (ERSSTv5): Upgrades, validations, and intercomparisons. J Climate 30: 8179-8205. https://doi.org/10.1175/JCLI-D-16-0836.1.

INPE. 2021. Meteorology Project of the Brazilian Antarctic Program. Available at http://antartica.cptec.inpe.br/. Accessed 03/Jul/2021.

KAYANO MT, ANDREOLI RV & SOUZA RAF. 2020. Pacific and Atlantic multidecadal variability relations to the El Niño events and their effects on the South American rainfall. Int J Climatol 40: 2183-2200. https://doi.org/10.1002/joc.6326.

KAYANO MT, ROSA MB, RAO VB, ANDREOLI RV & SOUZA RAF. 2019. Relations of the low-level extra-tropical cyclones in the Southeast Pacific and South Atlantic to the Atlantic multi-decadal oscillation. J Climate 34: 4167-4178. https://doi.org/10.1175/JCLI-D-18-0564.1.

KENDALL MG. 1975. Rank Correlation Methods, 4th ed., London: Charles Griffin Book Series, 272 p.

KERR RA. 2000. A North Atlantic climate pacemaker for the centuries. Science 288: 1984-1986. https://doi.org/10.1126/science.288.5473.1984.

KUCHARSKI F ET AL. 2016. Atlantic forcing of Pacific decadal variability. Clim Dyn 46: 2337-2351. https://doi.org/10.1007/s00382-015-2705-z.

LIM E-P & SIMMONDS I. 2002. Explosive cyclone development in the Southern Hemisphere and a comparison with Northern Hemisphere events. Mon Wea Rev 130: 2188-2209. https://doi.org/10.1175/1520-0493(2002)130<2188:ECDITS>2.0.CO;2.

LOPEZ H, DONG S, LEE S-K & CAMPOS E. 2016. Remote influence of interdecadal Pacific Oscillation on the South Atlantic meridional overturning circulation variability. Geophys Res Lett 43: 8250-8258. https://doi.org/10.1002/2016GL069067.

MANN HB. 1945. Nonparametric Tests Against Trend. Econometrica 13: 245-259. https://doi.org/10.2307/1907187.

MANTUA NJ, HARE SR, ZHANG Y, WALLACE JM & FRANCIS RC. 1997. A Pacific Interdecadal Climate Oscillation with Impacts on Salmon Production. Bull Amer Meteorol Soc 78: 1069-1079. https://doi.org/10.1175/1520-0477(1997)078<1069:APICOW>2.0.CO;2.

PACHAURI RK & MEYER LA. 2014. Climate Change 2014: Synthesis Report. Contribution of Working Groups I, II and III to the Fifth Assessment Report of the Intergovernmental Panel on Climate Change. Switzerland: IPCC, 151 p. https://www.ipcc.ch/site/assets/uploads/2018/05/SYR_AR5_FINAL_full_wcover.pdf (last access: February 21, 2021).

PANOFSKY HG & BRIER GW. 1968. Some applications of statistics to meteorology. Pennsylvania: Earth and Mineral Sciences Continuing Education, College of Earth and Mineral Sciences, Pennsylvania State University, 224 p.

PETTITT AN. 1979. A Non-Parametric Approach to the Change-Point Problem. J Roy Stat Soc. Ser C Appl Stat 28: 126-135. https://doi.org/10.2307/2346729.

REASON CJC & MURRAY RJ. 2001. Modelling low frequency variability in southern hemisphere extra-tropical cyclone characteristics and its sensitivity to sea-surface temperature. Int J Climatol 21: 249-267. https://doi.org/10.1002/joc.608.

ROMÃO M & SETZER A. 2008. Ciclones explosivos que atingiram Ferraz nos últimos 16 anos. XVI Simpósio de Pesquisa Antártica, Inst. Geociências, Centro de Pesquisas Antárticas, USP - Universidade de São Paulo, p. 90-91. Available at http://antartica.cptec.inpe.br/~rantar/publicacoes/200809_SPA_Romao_Setzer_ciclones_bomba.pdf. Accessed on 19/April/2021.

SANDERS F & GYAKUM JR. 1980. Synoptic–dynamic climatology of the "bomb." Mon Wea Rev 108: 1589-1606. https://doi.org/10.1175/1520-0493(1980)108<1589:SDCOT>2.0.CO;2.

SELUCHI ME & SAULO AC. 1998. Possible mechanisms yielding an explosive coastal cyclogenesis over South America: Experiments using a limited area model. Aust Meteor Mag 47: 309-320.

SEN PK. 1968. Estimates of the Regression Coefficient Based on Kendall's tau. J Amer Stat Assoc 63: 1379-1389.

SIMMONDS I & KEAY K. 2000. Mean Southern Hemisphere extratropical cyclone behavior in the 40-year NCEP–NCAR reanalysis. J Climate 13: 873-885. https://doi.org/10.1175/1520-0442(2000)013<0873:MSHECB>2.0.CO;2.

SINCLAIR MR. 1995. A climatology of cyclogenesis for the Southern Hemisphere. Mon Wea Rev 123: 1601-1619.

https://doi.org/10.1175/1520-0493(1995)123<1601:ACOCFT>2.0.CO;2.

SINCLAIR MR. 1997. Objective identification of cyclones and their circulation intensity, and climatology. Wea Forecasting 12: 595-612. https://doi.org/10.1175/1520-0434(1997)012<0595:OIOCAT>2.0.CO;2.

SPEER M, WILES P & PEPLER A. 2009. Low pressure systems off the New South Wales coast and associated hazardous weather: establishment of a database. Aust Meteor Oceanog J 58: 29-39. doi: 10.22499/2.5801.004.

THEIL H. 1950. A rank-invariant method of linear and polynomial regression analysis, 3; confidence regions for the parameters of polynomial regression equations. Indag Math 1: 467-482.

THEIL H. 1992. A Rank-Invariant Method of Linear and Polynomial Regression Analysis. In: RAJ B & KOERTS J (Eds), Henri Theil's Contributions to Economics and Econometrics. Advanced Studies in Theoretical and Applied Econometrics, Dordrecht: Springer, p. 345-381. https://doi.org/10.1007/978-94-011-2546-8_20.

TOFFOLI A & AERIA G. 2017. Exploring the birthplace of monster waves. Pursuit, The University of Melbourne, 14/Sept/2017.

TORRENCE C & WEBSTER PJ. 1999. Interdecadal changes in the ENSO monsoon system. J Climate 12: 2679-2690. https://doi.org/10.1175/1520-0442(1999)012%3C2679:ICITEM%3E2.0.CO;2.

WEC - WORLD ENVIRONMENTAL CONSERVANCY. 2021. Frei Antarctic Station – Explosive Cyclone – Apr/15/2021. Available at https://www.youtube.com/watch?v=MKKgkzRZcXk. Accessed 19/April/2021.

ALBERTO W. SETZER[1]
https://orcid.org/0000-0002-2466-7366

MARY T. KAYANO[1]
https://orcid.org/0000-0002-2516-295x

MARCELO R. OLIVEIRA[1, 2]
https://orcid.org/0000-0001-6332-035X

WILMAR L. CERÓN[3]
https://orcid.org/0000-0003-1901-9572

MARCELO B. ROSA[1]
https://orcid.org/0000-0002-0627-4876

[1]Coordenação Geral de Ciências da Terra,Instituto Nacional de Pesquisas Espaciais/ INPE, Av. dos Astronautas, 1758, 12227-010 São José dos Campos, SP, Brazil

[2]WEC- World Environmental Conservancy, PO Box 5987, Atlanta, GA 31107, USA

[3] Department of Geography, Faculty of Humanities, Universidad del Valle, 76001 Cali, Colombia

Correspondence to: **Alberto W. Setzer**
E-mail: alberto.setzer@inpe.br

Author contributions